Journal of Biomechanics ∎ (∎∎∎∎) ∎∎∎–∎∎∎

Contents lists available at ScienceDirect

Journal of Biomechanics

journal homepage: www.elsevier.com/locate/jbiomech
www.JBiomech.com

Non-invasive assessment of sciatic nerve stiffness during human ankle motion using ultrasound shear wave elastography

Ricardo J. Andrade [a,b], Antoine Nordez [a,*], François Hug [a,c], Filiz Ates [a], Michel W. Coppieters [c,d], Pedro Pezarat-Correia [b], Sandro R. Freitas [b]

[a] EA 4334, Laboratory "Movement, Interactions, Performance", University of Nantes, UFR STAPS, Nantes, France
[b] Universidade de Lisboa, Faculdade de Motricidade Humana, CIPER, P-1100 Lisbon, Portugal
[c] The University of Queensland, NHMRC Centre of Clinical Research Excellence in Spinal Pain, Injury and Health, School of Health and Rehabilitation Sciences, Brisbane, Australia
[d] MOVE Research Institute Amsterdam, Faculty of Behavioural and Movement Sciences, VU University Amsterdam, Amsterdam, The Netherlands

ARTICLE INFO

Article history:
Accepted 14 December 2015

Keywords:
Supersonic shear imaging
Shear wave velocity
Peripheral nerves
Sciatic nerve
Noninvasive mechanics

ABSTRACT

Peripheral nerves are exposed to mechanical stress during movement. However the *in vivo* mechanical properties of nerves remain largely unexplored. The primary aim of this study was to characterize the effect of passive dorsiflexion on sciatic nerve shear wave velocity (an index of stiffness) when the knee was in 90° flexion (knee 90°) or extended (knee 180°). The secondary aim was to determine the effect of five repeated dorsiflexions on the nerve shear wave velocity. Nine healthy participants were tested. The repeatability of sciatic nerve shear wave velocity was good for both knee 90° and knee 180° (ICCs $\geq$ 0.92, CVs $\leq$ 8.1%). The shear wave velocity of the sciatic nerve significantly increased ($p < 0.0001$) during dorsiflexion when the knee was extended (knee 180°), but no changes were observed when the knee was flexed (90°). The shear wave velocity–angle relationship displayed a hysteresis for knee 180°. Although there was a tendency for the nerve shear wave velocity to decrease throughout the repetition of the five ankle dorsiflexions, the level of significance was not reached ($p = 0.055$). These results demonstrate that the sciatic nerve stiffness can be non-invasively assessed during passive movements. In addition, the results highlight the importance of considering both the knee and the ankle position for clinical and biomechanical assessment of the sciatic nerve. This non-invasive technique offers new perspectives to provide new insights into nerve mechanics in both healthy and clinical populations (e.g., specific peripheral neuropathies).

1. Introduction

Peripheral nerves are exposed to significant mechanical stress during movement as they elongate and slide relative to adjacent tissues (Silva et al., 2014; Topp and Boyd, 2006). Furthermore, nerve excursion and strain are altered in people with peripheral neuropathies (Boyd and Dilley, 2014; Hough et al., 2007). As impaired nerve biomechanics is associated with compromised nerve function (Jou et al., 2000; Li and Shi, 2007; Rickett et al., 2011), a non-invasive quantification of the mechanical properties of peripheral nerves during movement may provide valuable information for the diagnosis and management of people with peripheral neuropathies.

The mechanical properties of peripheral nerves have been extensively examined in animal models (Kwan et al., 1992; Millesi et al., 1995), human cadaver studies (Boyd et al., 2013; Coppieters et al., 2006) and human *in vivo* studies (Boyd et al., 2012; Ellis et al., 2012). The majority of *in vivo* studies used ultrasound imaging to quantify nerve excursion and morphology (e.g., cross sectional area) (Beekman and Visser, 2004; Dilley et al., 2001; Silva et al., 2014). However, nerve excursion cannot be used to infer changes in stiffness or force. This is because the nerves may experience changes in their length within a slack length range (i.e., toe region of the load–elongation curve) while their stiffness or tension does not vary (Bueno and Shah, 2008; Coppieters and Butler, 2008; Topp and Boyd, 2006). Because of this limitation, the effects of joint motion on nerve stiffness and on tensile loads are largely unknown in *in vivo* situations. The influence of positions of neighbouring joints on nerve stiffness and tensile load

* Correspondence to: EA 4334, Laboratory "Movement, Interactions, Performance", University of Nantes, UFR STAPS, 25 bis Bd Guy Mollet, BP 72206, F-44000, Nantes, FRANCE.
E-mail address: antoine.nordez@univ-nantes.fr (A. Nordez).

http://dx.doi.org/10.1016/j.jbiomech.2015.12.017
0021-9290/

also remains largely unexamined. Finally, it is unclear whether repetitive loading or conditioning of the nerve affects its mechanical properties as is classically observed for other soft tissues such as skeletal muscles (McNair et al., 2002) and tendons (Maganaris, 2003).

Ultrasound shear wave elastography techniques, such as Supersonic Shear Imaging (SSI), measure the shear wave velocity within soft tissues (Bercoff et al., 2004). The shear wave velocity is directly linked to the shear modulus (Bercoff et al., 2004) and, thereby, can be used as a non-invasive metric of tissue stiffness (DeWall et al., 2014) and passive tension (Eby et al., 2013; Koo et al., 2013; Maisetti et al., 2012).

The primary aim of the present study was to characterize the effect of passive dorsiflexion on sciatic nerve shear wave velocity (an index of stiffness) when the knee was in 90° flexion (knee 90°) or extended (knee 180°). The secondary aim was to determine the effect of five repeated dorsiflexions on the nerve stiffness. To address these aims, we first needed to assess the reliability of shear wave velocity measurements for the sciatic nerve. Due to its particular mechanical relationship with knee and ankle joints, we hypothesized that the sciatic nerve stiffness would increase during both ankle dorsiflexion and knee extension.

2. Methods

2.1. Participants

Ten healthy males without low back or leg pain (mean (SD); age: 25.3 (2.5) years, height: 181.8 (6.9) cm, weight: 75.6 (7.5) kg) volunteered to participate in this study. Healthy individuals were selected as our intention was to reveal normal nerve biomechanics and to eliminate potentially confounding variables associated with dysfunction. Participants had no history of significant trauma or surgery to the spine, hip or hamstring region, or symptoms consistent with sciatic or tibial nerve pathology (e.g., pain, paraesthesias or weakness). The slump test [a test to assess the mechanosensitivity of the nervous system (Butler, 2000)] was negative in all participants. Participants had no known systemic disorders (e.g., diabetes) or signs of neurological conditions that might alter the function or morphology of the peripheral nervous system. The local ethics committee approved the study, and all the procedures were in agreement with the Declaration of Helsinki. Informed consent was obtained from all participants.

2.2. Experimental conditions

Shear wave velocity was measured within the sciatic nerve during passive ankle dorsiflexion with: *i*) knee in full extension (i.e., knee 180°); and *ii*) with the knee in 90° flexion (i.e., knee 90°). The ankle was passively moved from 40° of plantarflexion to 80% of the maximal range of dorsiflexion. The maximal range of dorsiflexion was defined as the angle corresponding to the onset of pain induced by the stretch of the plantar flexors.

An isokinetic dynamometer (Biodex 3 Medical, Shirley, NY, USA) was used to impose the ankle movements and determine the maximal range of motion (ROM). The neutral position (i.e., 0° of the ankle) was defined as an angle of 90° between the footplate of the dynamometer and the shank (i.e., foot perpendicular to the leg). This position was determined using an inclinometer. The lateral malleolus was aligned with the axis of the dynamometer and was considered as an estimate of the axis of rotation. Ankle angle data were collected at 1 kHz with an analogue/digital converter (ADInstruments, Powerlab 16/35, New Zealand). Positions of the hip (i.e., neutral) and knee were verified using a standard goniometer (MSD, Londerzeel, Belgium).

2.3. Elastography measurements

Shear wave velocity maps of the sciatic nerve were measured with an Aixplorer ultrasound scanner (Version 6.1; Supersonic Imagine, Aix-en-Provence, France) in shear wave elastography (SWE) mode (Bercoff et al., 2004) using the musculoskeletal (MSK) pre-set. A linear transducer (SL 10–2, Supersonic Imagine, Aix-en-Provence, France) was used. There was no temporal smoothing (persistence = OFF) and an intermediate spatial smoothing (5/9) was used. The maps of the shear wave velocity (Fig. 1, SWE-mode) were obtained at 1 sample/s with a spatial resolution of 1 × 1 mm.

First, the sciatic nerve was identified in the right posterior thigh ~7–10 cm distal to the gluteal fold using B-mode images (Bruhn et al., 2009, 2008; Karmakar et al., 2007). The probe was positioned perpendicular to the course of the sciatic nerve to obtain a cross sectional image (Fig. 1; B-mode Tv). At this level, the sciatic nerve is commonly an asymmetric structure. In order to obtain a representative value, the probe was centred over the thickest part of the nerve. The transducer was then rotated (90°) to acquire a longitudinal view of the sciatic nerve, and the SWE-mode was set. All ultrasound measurements were performed by an experienced examiner.

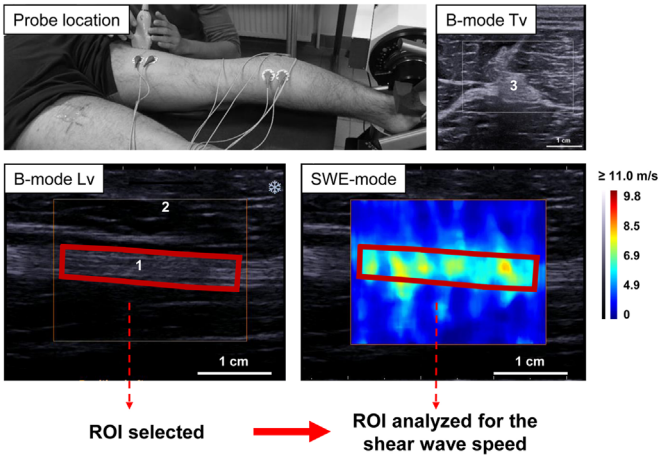

Fig. 1. Acquisition and processing of the maps of shear wave speed, First, the sciatic nerve was identified in the right posterior thigh ~7–10 cm distal to the gluteal fold using B-mode images. The probe was positioned perpendicular to the course of the sciatic nerve to obtain a cross sectional image (B-mode Tv). The transducer was then rotated (90°) to acquire a longitudinal view of the sciatic nerve (B-mode Lv). The region of interest (ROI) was determined from the B-mode image. The shear wave velocity data extracted from this ROI (SWE-mode) were averaged to obtain a representative value, legend: 1-Longitudinal view of sciatic nerve; 2-Long head of biceps femoris muscle. 3-Transverse view of sciatic nerve. Note: nerve fascicles are dark (hypoechoic) and nerve superficial bounds are defined by a hyperechoic structure (epineurium).

The location of the transducer was marked on the skin using a waterproof marker so that the transducer location remained constant across the tasks. A semi-rigid cable supported the manually held ultrasound transducer to reduce a possible motion of the transducer during the measurements.

Note that the shear wave velocity is reported in the present study, rather than the shear modulus as in previous muscle studies (Eby et al., 2013; Koo et al., 2013; Maisetti et al., 2012). In an infinite medium, the shear modulus (μ) can be directly calculated from the shear wave speed (Vs) using the following equation (Bercoff et al., 2004):

$$\mu = \rho V_s^2 \quad (1)$$

where ρ is the density of soft tissues (1000 k/gm^3). Using a shear wave dispersion analysis applied to Achilles tendon, Brum et al. (2014) showed that the shear wavelength (directly linked to the shear wave velocity) is longer than the tendon thickness. Therefore the wave propagation is guided because the medium cannot be considered as infinite. For this reason, recent tendon studies using SSI have reported shear wave velocity (DeWall et al., 2014; Slane et al., 2015). As shown in the present study, nerves are much less stiff than tendons and thus this issue is likely to be less problematic. However, as no study has applied the shear wave dispersion analysis to nerves, we chose to present our results as shear wave velocity.

2.4. Electromyography

Surface electromyography (EMG) was recorded to ensure that muscles were inactive during the elastography measurements. Surface electrodes (Kendall™ 100 Series Foam Electrodes, Covidien, Massachusetts, USA) were placed over the medial and lateral part of the gastrocnemius (MG and LG, respectively), tibialis anterior (TA), soleus (SOL) and semitendinosus (ST) muscles. Electrodes were placed according to the SENIAM recommendations [Surface EMG for Non-Invasive Assessment of Muscles (Hermens et al., 2000)] with an inter-electrode distance of 20 mm. Signals were amplified (× 1000) and digitized (8–500 Hz bandwidth) at a sampling rate of 1 kHz (ADInstruments, Powerlab 16/35, New Zealand). The root mean square of EMG signals (RMS-EMG, averaged over a time window of 300 ms) was calculated every seconds. Then, the RMS-EMG values were normalized to that recorded during maximal isometric voluntary contraction (MVIC).

2.5. Data collection and analysis

Five conditioning cycles of passive ankle dorsiflexion and plantarflexion were first performed. These trials were conducted to evaluate a possible conditioning effect of the ankle movements on sciatic nerve mechanical properties during the initial loading–unloading cycles. The conditioning cycles were performed at 5°/s. Three post-conditioning loading and unloading motions were performed at 2°/s to measure the effect of ankle position on sciatic nerve stiffness and to calculate the reliability of the nerve shear wave speed measurement. The measurements were

Please cite this article as: Andrade, R.J., et al., Non-invasive assessment of sciatic nerve stiffness during human ankle motion using ultrasound shear wave elastography. Journal of Biomechanics (2015), http://dx.doi.org/10.1016/j.jbiomech.2015.12.017

randomly performed with the knee in flexion (knee 90°) and extension (knee 180°), and there was a 5-min rest period between experimental conditions.

Maps of the shear wave velocity were processed using a custom Matlab script (The Mathworks, Natick, USA). The region-of-interest (ROI) was first determined in the B-mode image by selecting the largest area in accordance with nerve boundaries (Fig. 1, B-mode Lv). Because the sciatic nerve moves in an antero-posterior direction during ankle movement (Boyd et al., 2012), the ROI was manually adjusted for each frame (i.e., each second). The shear wave velocity data extracted from this ROI were averaged to obtain a representative value. Each map was visually inspected for saturated values, i.e., values that reached the maximal measurable shear wave velocity (14.1 m/s for the version of the SSI device we used). When observed, these regions of saturated values did not consistently appear on all measurements (i.e., elasticity maps) making us think that they were artifacts related to measurement rather than true regions of high stiffness. As a result of this inspection, one participant was excluded and therefore data from the remaining 9 participants were analyzed.

For the first post-conditioning cycle, the area under the shear wave velocity–ankle angle load curve, the area under the unload curve, and the normalized hysteresis area were calculated as described by Nordez et al. (2008).

As the maximum ROM varied between participants, the ankle angle was normalized to the maximal ROM. Zero percent was defined as the starting position (i.e., 40° of plantarflexion) and 100% as the end position (i.e., 80% of maximum ankle dorsiflexion). Shear wave velocity, ankle angle and EMG data were synchronised by recording a trigger from the ultrasound device (ADInstruments, Powerlab 16/35, New Zealand). Synchronised data were analyzed for the first and fifth conditioning cycles, and for the three post-conditioning cycles performed at 2°/s. Linear interpolation was used to calculate the shear wave velocity every 2° of ankle angle in order to combine it with mechanical data.

2.6. Statistics

The IBM SPSS software (version 20.0; IBM Corporation, New York, USA) was used for the statistics procedures. Distributions consistently passed the Kolmogorov–Smirnov normality test. All data are reported as mean ± standard deviation (SD).

The reliability of the shear wave velocity was determined across the 3 post-conditioning repetitions, at three ankle angles (20° dorsiflexion; neutral position (0°); and 20° plantarflexion) for both knee conditions during the loading phase (ankle dorsiflexion). The interclass coefficient correlation ($ICC_{[2,1]}$), standard error of measurement (SEM), and coefficient of variation (CV) were calculated (Hopkins, 2000).

To test whether the effect of ankle movements on nerve shear wave velocity was different between the two knee positions a two-way repeated-measures ANOVA was conducted on data from the first post-conditioning cycle [within-subject factors: Ankle angle with 11 levels (0–100% of total ROM with 10% increments) and Knee position with 2 levels (knee 90° and knee 180°)]. To determine whether a hysteresis occurred, a comparison between the areas under the load curve and unload curves of the shear wave velocity–ankle angle relationships was performed for both knee 180° and knee 90° using two separate paired *T*-tests.

To test the effect of repeated ankle passive movements on the sciatic nerve shear wave velocity a repeated measures ANOVA was performed for knee 180° condition only [within-subject factors: Ankle angle with 11 levels (0–100% of total ROM with 10% increments) and Cycle with 2 levels (1st and 5th cycle)].

Post-hoc analyses were performed when appropriated using Bonferroni correction method for multiple comparisons. The statistical significance was set at $p < 0.05$.

3. Results

The normalized RMS-EMG values remained lower than 1% of MVC for all the examined muscles (MG, LG, TA, SOL and ST) and participants allowing us to consider that the ankle dorsiflexions were performed in a passive state. A typical example of the shear wave velocity *vs* ankle angle relationship is depicted in Fig. 2. The repeatability of the nerve shear wave velocity was good at each ankle angle for both experimental conditions (i.e., knee 180° and the knee 90°). All SEM and CV values were lower than 0.34 m/s and 8.1%, respectively (Table 1). All ICC values were higher than 0.92 (Table 1).

There was a significant main effect of both ankle angle ($p < 0.0001$) and knee position ($p < 0.0001$) on nerve shear wave velocity. A significant interaction between ankle angle and knee position was also found ($p < 0.0001$) showing that although nerve shear wave velocity increased with ankle dorsiflexion for knee 180°, no changes were observed for knee 90°. Consequently, the nerve shear wave velocity was significantly higher for knee 180° than knee 90° at each ankle angle (all p values ≤ 0.001; Fig. 3). For knee 180°, the shear wave velocity was significantly higher at 70%, 80%, 90% and 100% of ankle angle relative to 0% (p values ≤ 0.002). For knee 90°, no significant changes in shear wave velocity were observed for any ankle angles compared to the 0% value (p values ≥ 0.056). The average increase of shear wave velocity was 33.7 ± 9.4% (range: 25.4–47.4% for 0% and 100% of ankle motion, respectively). For example, at 100% of ankle ROM shear wave velocity was 10.4 ± 2.4 and 5.3 ± 1.1 m/s for knee 180° and knee 90°, respectively.

When the knee was at 180°, the area under the loading curve was significantly higher ($p=0.001$) than the area under the unloading curve during the first ankle motion (Fig. 4). The normalized hysteresis area was 9.5 ± 5.2%. No significant difference ($p=0.58$) was found when the knee was at 90° (average difference: −0.3 ± 2.0%).

Although a main effect of ankle angle ($p=0.0001$) was found (similar to that reported above), neither a main effect of Cycle ($p=0.055$) nor an interaction between ankle angle and cycle ($p=0.340$) were found for the five conditioning ankle cycles.

4. Discussion

We investigated the shear wave velocity (an index of stiffness) of the sciatic nerve during passive ankle rotation at two knee angles. The present study shows that: *i*) SSI provides a reliable *in vivo* measurement of sciatic nerve shear wave velocity during ankle rotation; *ii)* sciatic nerve shear wave velocity increases with the ankle dorsiflexion, but this is only observed when the knee is extended at 180°; and *iii)* there was a tendency for the sciatic nerve shear wave velocity to decrease throughout the repetition of the five repeated ankle rotation motions.

A high reproducibility of SSI measurements has been previously observed in the median nerve, however only in resting conditions (Kantarci et al., 2014). Our results showed a good repeatability of the sciatic shear wave velocity measured at the proximal third of the thigh during passive and slow ankle movements (Table 1). These results highlight the potential of using shear wave elastography to non-invasively evaluate the mechanical properties of peripheral nerves at rest and during passive stretching.

The sciatic nerve stiffness increased substantially during dorsiflexion for the knee 180° condition, but no changes were observed when the knee was flexed (knee 90°) (Fig. 3). These observations are in line with previous studies, which showed that ankle dorsiflexion was associated with distal excursion of the sciatic nerve and its corresponding tibial branch (Coppieters et al., 2006). Taken together, these results show that sciatic nerve tension increases when is stretched due to specific positioning of multiple joints that the sciatic nerve crosses. This mechanical tensile response has already been shown in animal and *in vitro* studies (Silva et al., 2014; Topp and Boyd, 2006). Moreover, mechanical forces acting on peripheral nerves are thought to be transmitted well beyond the moving joint (Coppieters et al., 2006; Coppieters and Butler, 2008). Thus, the anatomical features of the sciatic nerve may explain the absence of stiffness changes during ankle rotation when the knee was flexed at 90°. The sciatic nerve (i.e., tibial and peroneal related branches) runs along the popliteal crease just behind the sagittal axis of rotation of the knee (Vloka et al., 2001). Therefore, when the knee is flexed, the structures crossing the joint may fold and slacken the nerve. Further investigations are needed to determine the effects of the cumulative nerve tensioning that may be induced by the position of the joints that it crosses.

In the present study the measurements of nerve stiffness were performed proximally, therefore at relatively large distance from

Please cite this article as: Andrade, R.J., et al., Non-invasive assessment of sciatic nerve stiffness during human ankle motion using ultrasound shear wave elastography. Journal of Biomechanics (2015), http://dx.doi.org/10.1016/j.jbiomech.2015.12.017

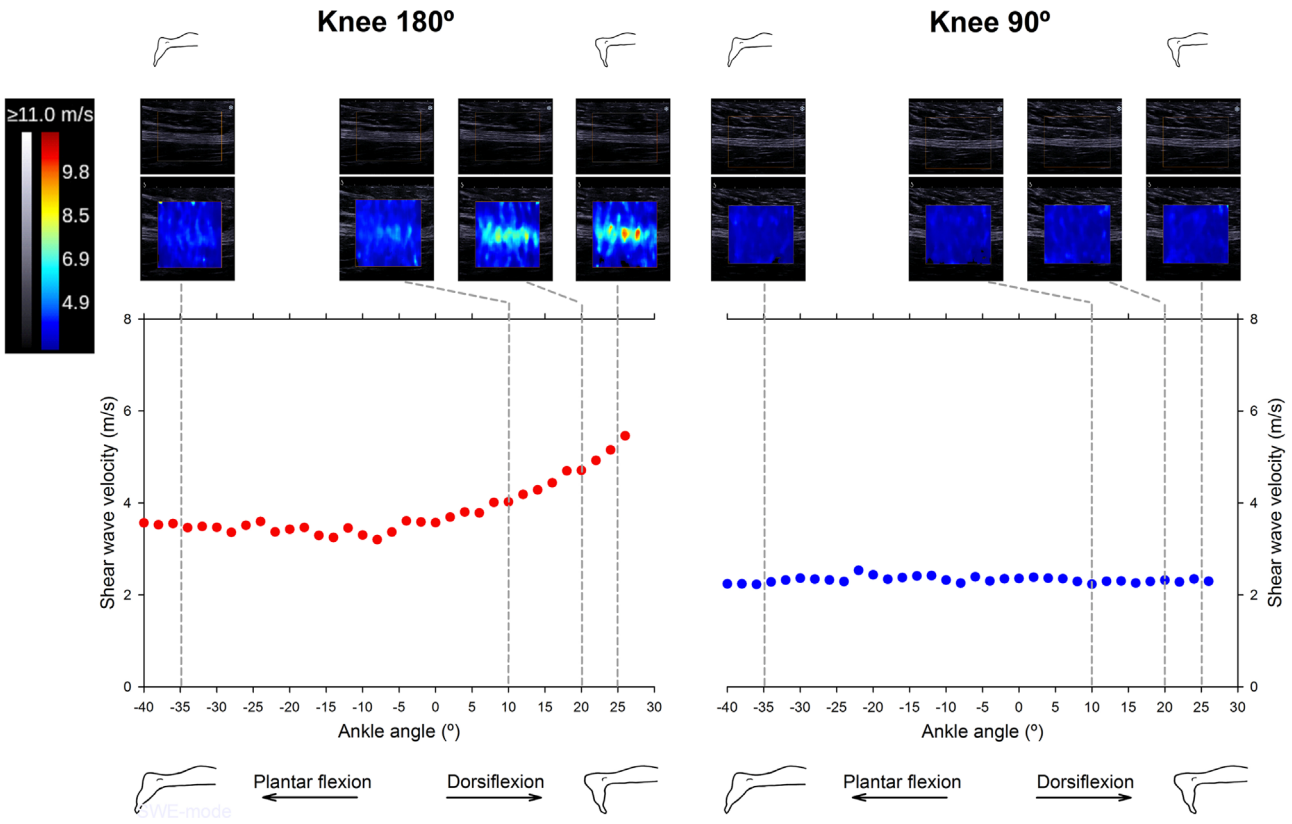

Fig. 2. Typical example of the nerve shear wave velocity during passive ankle dorsiflexion for both experimental conditions. Knee 180° – relationship between ankle angle and shear wave velocity with the knee fully extended. Knee 90° – relationship between ankle angle and shear wave velocity with the knee flexed. The upper panels correspond to the shear wave velocity maps obtained at −35°, 10°, 20° and 25° of ankle dorsiflexion.

Table 1
Repeatability of the sciatic shear wave velocity for both experimental conditions (knee 180° and knee 90°) at three ankle angles. ICC – Interclass correlation coefficient; SEM – Standard error of measurement; CV – Coefficient of variation.

Ankle position	Knee 180°			Knee 90°		
	ICC (95%CI)	SEM (m/s)	CV (%)	ICC (CI)	SEM (m/s)	CV (%)
Plantar flexion (−20°)	0.97 [0.90;0.99]	0.21	5.0	0.98 [0.93;1.00]	0.17	2.9
Neutral	0.98 [0.93;1.00]	0.17	4.0	0.97 [0.89;0.99]	0.21	4.5
Dorsiflexion (20°)	0.99 [0.95;1.00]	0.14	3.6	0.92 [0.72;0.98]	0.34	8.1

the moved ankle joint. Nerve architecture is different between joint and non-joint areas (Phillips et al., 2004). Moreover, an *in situ* animal study showed that the nerve regions near the joints undergo greater elongation than other regions during joint movement (Phillips et al., 2004). Together, these observations suggest that the interpretation of our results should be confined to the specific location where the stiffness was measured. Further studies are needed to characterize the spatial variability of nerve stiffness behaviour during limb movements.

Our results showed that there is a tendency for the nerve shear wave velocity to decrease throughout the repetition of five ankle rotations, despite the level of statistical significance not being reached ($p=0.055$). This lack of significance is likely explained by a lack of statistical power associated to our small sample size. In a previous *in situ* animal study, cyclic sciatic nerve stretching was performed at different pre-strain levels (i.e., induced by an end-to-end anastomosis surgical approach) (Orf and Wust, 1979). The

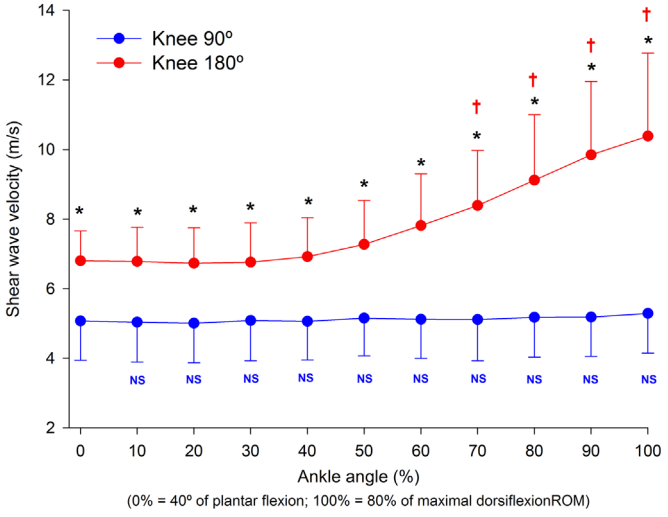

Fig. 3. Shear wave velocity and ankle angle relationship for both experimental conditions. 0% of ankle angle = starting test position (40° of ankle plantarflexion); 100% of ankle dorsiflexion angle = 80% of maximal dorsiflexion angle. *Shear wave velocity was significantly greater for knee 180° *vs* knee 90° across all ankle angle increments (every 10% from 0% to 100%): p values ranging from 0.001 to 0.002. † For knee 180°, shear wave velocity was significantly higher at 70%, 80%, 90% and 100% relative to the 0% of ankle angle: p values ranging from 0.001 to 0.002. NS For knee 90°, there were no significant differences between the 0% and all other ankle angles increments (from 10% to 100%): p values higher than 0.056.

repetitive nerve stretching did not alter the stress–strain curves when the nerve was pre-strained below 8% of the initial nerve length. However, for higher pre-strained levels (i.e., 8% and 10% of the initial nerve length) a significant effect of repeated joint rotation was found. It is therefore possible that further stretch

Please cite this article as: Andrade, R.J., et al., Non-invasive assessment of sciatic nerve stiffness during human ankle motion using ultrasound shear wave elastography. Journal of Biomechanics (2015), http://dx.doi.org/10.1016/j.jbiomech.2015.12.017

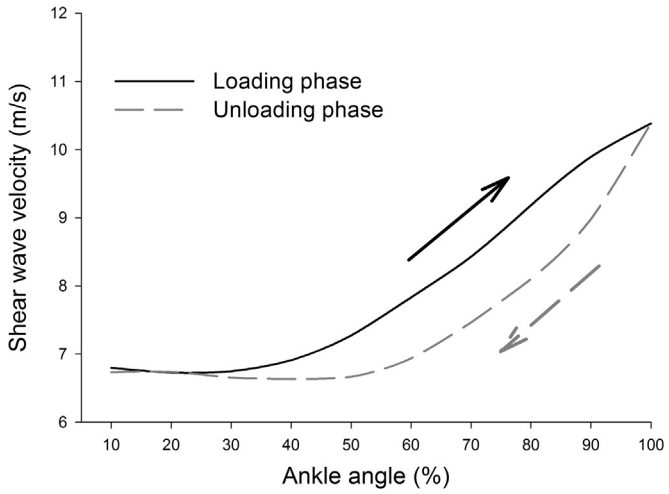

Fig. 4. Averaged load and unload curves (shear wave velocity of sciatic nerve) during ankle passive movement for knee extended (knee 180°) condition. 0% corresponds to 40° of plantarflexion and 100% to 80% of maximum dorsiflexion. The normalized hysteresis area was calculated as Nordez et al. (2008). Knee 90° was not represented due to a lack of changes in load and unload curves.

applied to the sciatic nerve (e.g., by changing the hip position or by stretching the ankle to $>80\%$ of maximal ROM) might have induced a significant effect of loading cycles on nerve stiffness.

The area under the loading curve was significantly higher than the area under the unloading curve when the knee was extended (knee 180°). This indicates the presence of a hysteresis, which was expected as the nerve is a viscoelastic tissue (Topp and Boyd, 2006). Although this result is in accordance with previous *in situ* and *in vitro* studies (Chen et al., 2010; Ju et al., 2006; Rickett et al., 2011), it was not demonstrated *in vivo* so far. The absence of hysteresis observed in knee 90° is likely explained by the lack of tensioning of proximal region of the sciatic nerve during ankle dorsiflexion (i.e., no loading).

There are a couple of methodological issues that have to be discussed and addressed in the future works. First, a spatial variability of shear wave velocity was observed (e.g. nerve maps at 20° and 25° on Fig. 2 – Knee 180°). Similar observations were reported from stretched muscles (Freitas et al., 2015; Le Sant et al., 2015) or tendons (Hug et al., 2013). This variability is likely related to the variability in both architecture and composition of these tissues. To limit the influence of this variability on our results, the shear wave velocity values were averaged over a representative ROI that remained the same throughout the entire ankle ROM. Second, as observed in the B-mode image of the Fig. 1 (transverse view), the sciatic nerve has an asymmetric architecture. It is unknown whether this asymmetry is related to a spatial variability of its mechanical properties. Because the spatial resolution of the SSI technique is limited to $1 \times 1\ mm^2$ and because the nerve is a thin structure, this variability could not be assessed in our study.

Finally, there is evidence that nerve mechanical properties influences both the efficiency of nerve functions and the protection of the nerve fascicles (Topp and Boyd, 2006). For example, the amplitude of the compound action potential decreases linearly as the nerve strain increases (Li and Shi, 2007; Rickett et al., 2011; Wall et al., 1992). Furthermore, it is particularly important to consider that changes in nerve morphology can be triggered by pathophysiological processes [e.g., modifications in collagen content, fibril diameter, cross sectional area and intraneural pressure (Di Pasquale et al., 2015; Goedee et al., 2013; Topp and Boyd, 2006)], and therefore are likely to affect nerve tension and stiffness during movements. Consequently, the non-invasive characterization of the nerve mechanical properties proposed in the present study may be clinically relevant to allow the clinician to: 1) diagnose a pathological nerve; 2) design appropriate treatment techniques based on manual therapy (i.e., neural tension *vs* neural excursion); and 3) have real-time feedback of the intervention minimizing the physical stress that is induced on the injured nerve.

5. Conclusion

In summary, we showed that the shear wave velocity (an index of stiffness) of the sciatic nerve can be experimentally assessed during slow passive ankle rotation using SSI. In addition, this study demonstrates that the shear wave velocity of the sciatic nerve is influenced by the knee position regardless of the ankle joint, suggesting a cumulative tensioning effect of the nerve induced by the position of multiple joints. An increase in nerve shear wave velocity during ankle dorsiflexion was observed only when the knee was extended. Finally, the nerve shear wave velocity was not affected by five stretching repetitions. This is the first study that non-invasively assesses nerve stiffness during a joint movement. The notable dependence of the sciatic tension on nerve mechanics induced by the joints' positioning, which the nerve crosses, should be considered during clinical assessment and interventions (e.g., to minimize physical stress on an injured nerve). Further investigations are therefore required to characterize the peripheral nerves mechanics during joints movement, in both healthy and clinical populations (e.g., specific peripheral neuropathies).

Conflict of interest

The authors have no conflict of interest.

Acknowledgements

This study was supported by grants from the European Regional development Fund (ERDF, no. 37400) and the Region Pays de la Loire (QUETE project, no. 2015-09035).

References

Beekman, R., Visser, L.H., 2004. High-resolution sonography of the peripheral nervous system – a review of the literature. Eur. J. Neurol. 11, 305–314.
Bercoff, J., Tanter, M., Fink, M., 2004. Supersonic shear imaging: a new technique for soft tissue elasticity mapping. IEEE Trans. Ultrason. Ferroelectr. Freq. Control 51, 396–409.
Boyd, B.S., Dilley, A., 2014. Altered tibial nerve biomechanics in patients with diabetes mellitus. Muscle Nerve 50, 216–223.
Boyd, B.S., Gray, A.T., Dilley, A., Wanek, L., Topp, K.S., 2012. The pattern of tibial nerve excursion with active ankle dorsiflexion is different in older people with diabetes mellitus. Clin. Biomech. 27, 967–971.
Boyd, B.S., Topp, K.S., Coppieters, M.W., 2013. Impact of movement sequencing on sciatic and tibial nerve strain and excursion during the straight leg raise test in embalmed cadavers. J. Orthop. Sports Phys. Ther. 43, 398–403.
Bruhn, J., Moayeri, N., Groen, G.J., A, V.A.N.V., Gielen, M.J., Scheffer, G.J., GJ,, V.A.N.G., 2009. Soft tissue landmark for ultrasound identification of the sciatic nerve in the infragluteal region: the tendon of the long head of the biceps femoris muscle. Acta Anaesthesiol. Scand. 53, 921–925.
Bruhn, J., Van Geffen, G.J., Gielen, M.J., Scheffer, G.J., 2008. Visualization of the course of the sciatic nerve in adult volunteers by ultrasonography. Acta Anaesthesiol. Scand. 52, 1298–1302.
Brum, J., Bernal, M., Gennisson, J.L., Tanter, M., 2014. In vivo evaluation of the elastic anisotropy of the human Achilles tendon using shear wave dispersion analysis. Phys. Med. Biol. 59, 505–523.
Bueno, F.R., Shah, S.B., 2008. Implications of tensile loading for the tissue engineering of nerves. Tissue Eng. Part B Rev. 14, 219–233.
Butler, D.S., 2000. The Sensitive Nervous System. Noigroup Publications, Adelaide, Australia.
Chen, R.J., Lin, C.C., Ju, M.S., 2010. In situ transverse elasticity and blood perfusion change of sciatic nerves in normal and diabetic rats. Clin. Biomech. 25, 409–414.

Coppieters, M.W., Alshami, A.M., Babri, A.S., Souvlis, T., Kippers, V., Hodges, P.W., 2006. Strain and excursion of the sciatic, tibial, and plantar nerves during a modified straight leg raising test. J. Orthop. Res. 24, 1883–1889.
Coppieters, M.W., Butler, D.S., 2008. Do'sliders' slide and'tensioners' tension? An analysis of neurodynamic techniques and considerations regarding their application. Man. Ther. 13, 213–221.
DeWall, R.J., Slane, L.C., Lee, K.S., Thelen, D.G., 2014. Spatial variations in Achilles tendon shear wave speed. J. Biomech. 47, 2685–2692.
Di Pasquale, A., Morino, S., Loreti, S., Bucci, E., Vanacore, N., Antonini, G., 2015. Peripheral nerve ultrasound changes in CIDP and correlations with nerve conduction velocity. Neurology 84, 803–809.
Dilley, A., Greening, J., Lynn, B., Leary, R., Morris, V., 2001. The use of cross-correlation analysis between high-frequency ultrasound images to measure longitudinal median nerve movement. Ultrasound Med. Biol. 27, 1211–1218.
Eby, S.F., Song, P., Chen, S., Chen, Q., Greenleaf, J.F., An, K.N., 2013. Validation of shear wave elastography in skeletal muscle. J. Biomech. 46, 2381–2387.
Ellis, R.F., Hing, W.A., McNair, P.J., 2012. Comparison of longitudinal sciatic nerve movement with different mobilization exercises: an in vivo study utilizing ultrasound imaging. J. Orthop. Sports Phys. Ther. 42, 667–675.
Freitas, S.R., Andrade, R.J., Larcoupaille, L., Mil-homens, P., Nordez, A., 2015. Muscle and joint responses during and after static stretching performed at different intensities. Eur. J. Appl. Physiol. 115, 1263–1272.
Goedee, H.S., Brekelmans, G.J., van Asseldonk, J.T., Beekman, R., Mess, W.H., Visser, L.H., 2013. High resolution sonography in the evaluation of the peripheral nervous system in polyneuropathy–a review of the literature. Eur. J. Neurol. 20, 1342–1351.
Hermens, H.J., Freriks, B., Disselhorst-Klug, C., Rau, G., 2000. Development of recommendations for SEMG sensors and sensor placement procedures. J. Electromyogr. Kinesiol. 10, 361–374.
Hopkins, W.G., 2000. Measures of reliability in sports medicine and science. Sports Med. 30, 1–15.
Hough, A.D., Moore, A.P., Jones, M.P., 2007. Reduced longitudinal excursion of the median nerve in carpal tunnel syndrome. Arch. Phys. Med. Rehabil. 88, 569–576.
Hug, F., Lacourpaille, L., Maisetti, O., Nordez, A., 2013. Slack length of gastrocnemius medialis and Achilles tendon occurs at different ankle angles. J. Biomech. 46, 2534–2538.
Jou, I.M., Lai, K.A., Shen, C.L., Yamano, Y., 2000. Changes in conduction, blood flow, histology, and neurological status following acute nerve-stretch injury induced by femoral lengthening. J. Orthop. Res. 18, 149–155.
Ju, M.S., Lin, C.C., Fan, J.L., Chen, R.J., 2006. Transverse elasticity and blood perfusion of sciatic nerves under in situ circular compression. J. Biomech. 39, 97–102.
Kantarci, F., Ustabasioglu, F.E., Delil, S., Olgun, D.C., Korkmazer, B., Dikici, A.S., Tutar, O., Nalbantoglu, M., Uzun, N., Mihmanli, I., 2014. Median nerve stiffness measurement by shear wave elastography: a potential sonographic method in the diagnosis of carpal tunnel syndrome. Eur. Radiol. 24, 434–440.
Karmakar, M.K., Kwok, W.H., Ho, A.M., Tsang, K., Chui, P.T., Gin, T., 2007. Ultrasound-guided sciatic nerve block: description of a new approach at the subgluteal space. Br. J. Anaesth. 98, 390–395.
Koo, T.K., Guo, J.Y., Cohen, J.H., Parker, K.J., 2013. Relationship between shear elastic modulus and passive muscle force: an ex-vivo study. J. Biomech. 46, 2053–2059.
Kwan, M.K., Wall, E.J., Massie, J., Garfin, S.R., 1992. Strain, stress and stretch of peripheral nerve. Rabbit experiments in vitro and in vivo. Acta Orthop. Scand. 63, 267–272.
Le Sant, G., Ates, F., Brasseur, J.L., Nordez, A., 2015. Elastography study of hamstring behaviors during passive stretching. PloS One 10, e0139272.
Li, J., Shi, R., 2007. Stretch-induced nerve conduction deficits in guinea pig ex vivo nerve. J. Biomech. 40, 569–578.
Maganaris, C.N., 2003. Tendon conditioning: artefact or property? Proc. Biol. Sci. 270 (Suppl 1), S39–S42.
Maisetti, O., Hug, F., Bouillard, K., Nordez, A., 2012. Characterization of passive elastic properties of the human medial gastrocnemius muscle belly using supersonic shear imaging. J. Biomech. 45, 978–984.
McNair, P.J., Hewson, D.J., Dombroski, E., Stanley, S.N., 2002. Stiffness and passive peak force changes at the ankle joint: the effect of different joint angular velocities. Clin. Biomech. 17, 536–540.
Millesi, H., Zoch, G., Reihsner, R., 1995. Mechanical properties of peripheral nerves. Clin. Orthop. Relat. Res., 76–83.
Nordez, A., McNair, P., Casari, P., Cornu, C., 2008. Acute changes in hamstrings musculo-articular dissipative properties induced by cyclic and static stretching. Int. J. Sports Med. 29, 414–418.
Orf, G., Wust, R., 1979. Mechanical loading of peripheral nerves during remobilisation of the affected member after end-to-end anastomosis. Acta Neurochir. 49, 103–121.
Phillips, J.B., Smit, X., De Zoysa, N., Afoke, A., Brown, R.A., 2004. Peripheral nerves in the rat exhibit localized heterogeneity of tensile properties during limb movement. J. Physiol. 557, 879–887.
Rickett, T., Connell, S., Bastijanic, J., Hegde, S., Shi, R., 2011. Functional and mechanical evaluation of nerve stretch injury. J. Med. Syst. 35, 787–793.
Silva, A., Manso, A., Andrade, R., Domingues, V., Brandao, M.P., Silva, A.G., 2014. Quantitative in vivo longitudinal nerve excursion and strain in response to joint movement: a systematic literature review. Clin. Biomech. 29, 839–847.
Slane, L.C., DeWall, R., Martin, J., Lee, K., Thelen, D.G., 2015. Middle-aged adults exhibit altered spatial variations in Achilles tendon wave speed. Physiol. Meas. 36, 1485–1496.
Topp, K.S., Boyd, B.S., 2006. Structure and biomechanics of peripheral nerves: nerve responses to physical stresses and implications for physical therapist practice. Phys. Ther. 86, 92–109.
Vloka, J.D., Hadzic, A., April, E., Thys, D.M., 2001. The division of the sciatic nerve in the popliteal fossa: anatomical implications for popliteal nerve blockade. Anesth. Analg. 92, 215–217.
Wall, E.J., Massie, J.B., Kwan, M.K., Rydevik, B.L., Myers, R.R., Garfin, S.R., 1992. Experimental stretch neuropathy. Changes in nerve conduction under tension. J. Bone Joint Surg. Br. 74, 126–129.

Please cite this article as: Andrade, R.J., et al., Non-invasive assessment of sciatic nerve stiffness during human ankle motion using ultrasound shear wave elastography. Journal of Biomechanics (2015), http://dx.doi.org/10.1016/j.jbiomech.2015.12.017